SPANDIDOS PUBLICATIONS

ONCOLOGY REPORTS 50: 164, 2023

Upregulation of integrin-linked kinase enhances tumor progression in gemcitabine-resistant pancreatic cancer

HIROMICHI MURASE, YOICHI MATSUO, YUKI DENDA, KEISUKE NONOYAMA, TOMOKATSU KATO, YOSHINAGA AOYAMA, YUICHI HAYASHI, HIROYUKI IMAFUJI, KENTA SAITO, MAMORU MORIMOTO, RYO OGAWA, HIROKI TAKAHASHI, AKIRA MITSUI, MASAHIRO KIMURA and SHUJI TAKIGUCHI

Department of Gastroenterological Surgery, Nagoya City University Graduate School of Medical Sciences, Mizuho-cho, Mizuho-ku, Nagoya, Aichi 4678601, Japan

Received February 13, 2023; Accepted May 18, 2023

DOI: 10.3892/or.2023.8601

Abstract. Pancreatic cancer (PaCa) tends to be resistant to chemotherapy and is associated with a very poor prognosis. It has been previously reported by the authors that integrin-linked kinase (ILK) is a prognostic factor in PaCa. ILK expression was examined in a newly established gemcitabine (Gem)-resistant (Gem-R) PaCa cell line and it was demonstrated that ILK expression was upregulated compared with that in Gem-sensitive (Gem-S) cells. In the present study, the effects of increased ILK expression in Gem-R PaCa cells were evaluated and it was examined whether compound 22 (Cpd22), an ILK inhibitor, exerted antitumor effects not only in Gem-S cells but also in Gem-R cells. Reverse transcription-quantitative polymerase chain reaction and western blotting revealed that ILK expression was higher in Gem-R PaCa cells than in Gem-S PaCa cells. Cpd22 inhibited the growth of PaCa cells in a concentration-dependent manner. Cpd22 also inhibited the growth of Gem-R PaCa cells. The invasive and angiogenic potential of Gem-R PaCa cells was enhanced compared with that in Gem-S cells; however, ILK small interfering RNA and Cpd22 treatment suppressed this enhancement of invasive potential compared with that in Gem-S cells. The addition of Cpd22 to Gem also improved the sensitivity of Gem-R cell lines to Gem. Furthermore, enhanced Akt signaling was associated with increased malignancy in Gem-R cell lines. In conclusion, ILK was upregulated with resistance and may be involved in tumor angiogenesis, invasive potential, and chemotherapy resistance, which were all suppressed by Cpd22 treatment. Thus, Cpd22 may be a novel therapeutic agent for the treatment of PaCa.

Correspondence to: Dr Yoichi Matsuo, Department of Gastroenterological Surgery, Nagoya City University Graduate School of Medical Sciences, 1 Kawasumi, Mizuho-cho, Mizuho-ku, Nagoya, Aichi 467-8601, Japan
E-mail: matsuo@med.nagoya-cu.ac.jp

Key words: integrin-linked kinase, gemcitabine-resistance, integrin-linked kinase inhibitor, compound 22, pancreatic cancer

Introduction

Pancreatic cancer (PaCa) is a type of gastrointestinal cancer that is relatively resistant to treatment; accordingly, the prognosis of patients with PaCa is poor. In both Japan and the United States of America, PaCa is the fourth leading cause of cancer-related deaths, and the number of deaths is increasing every year (1). Multidisciplinary treatments combining surgery, chemotherapy, and radiotherapy have recently been developed to treat PaCa. In the past 10 years, with advances in treatment methods, the 5-year survival rate of patients with PaCa has increased from 6 to 11%, although it is still far from satisfactory (1). One of the main reasons for this lack of efficacy is that PaCa readily becomes resistant to chemotherapy.

Gemcitabine (Gem) has been used to treat PaCa since 1977 (2) and is still a key drug used as both adjuvant chemotherapy (3) and in Gem plus nab-paclitaxel (GnP) combination treatment for distant metastases (4). Therefore, Gem resistance in PaCa is a major clinical problem, and the identification of factors associated with Gem resistance and the development of therapies targeting these factors are necessary to improve prognoses. Some studies have discovered the importance of integrin-linked kinase (ILK) in chemoresistance (5,6). A previous study by the authors revealed similar findings and demonstrated that ILK is important, even after its effect on Gem becomes inadequate. ILK is an intracellular effector related to cell-matrix interactions and is associated with multiple signaling pathways, including AKT, glycogen synthase kinase (GSK)-3β (7). In cancer tissues, ILK is often upregulated, suggesting that ILK contributes to proliferation, invasion, angiogenesis, and metastasis (8,9). Therefore, downregulation of downstream signaling pathways via suppression of ILK may play a major role in cancer control, and ILK-targeted therapies are being developed for numerous cancer types (9-12). Previous research has described the efficacy of ILK inhibitors in PaCa (13). However, no functional analyses of ILK have been reported in established Gem-resistant (Gem-R) cell lines, and the antitumor effects of ILK inhibitors in Gem-R cell lines have not been elucidated. ILK has been demonstrated to be involved in chemotherapy resistance by promoting apoptosis and the epithelial-mesenchymal transition (EMT) (5,6,14). However, in these studies, ordinary cancer cells were used.

Therefore, in the present study, the role of ILK was evaluated using a Gem-R PaCa cell line that was established by the authors, originally. Preliminary experiments revealed that ILK expression was upregulated in this Gem-resistant cell line compared to the Gem-S PaCa cell line. Therefore, it was determined how the increased expression of ILK affects the behavior of the Gem-R PaCa-resistant lines. The effect of ILK inhibitors on PaCa cell lines was also investigated, including the Gem-R PaCa cell lines.

Materials and methods

Reagents. Compound 22 (Cpd22, $C_{30}H_{30}F_3N_5O$) and dimethyl sulfoxide (DMSO) were purchased from Sigma-Aldrich (Merck KGaA). Cpd22 was dissolved in DMSO at 50 mM and used as a stock solution. The solution was aliquoted into 200-μl tubes and stored at -20˚C. GSK690693 was purchased from Selleck Chemicals.

Establishment of Gem-R PaCa cell lines. In this experiment, Gem-R PaCa cell lines were utilized that had been previously established by the authors, originally (15). The method of establishment is briefly described below. The half maximal inhibitory concentration (IC_{50}) of GEM against parental MIA PaCa-2 or AsPC-1 cells was determined using WST-1 assay. The IC_{50} of GEM for each PaCa cell line was established by constructing a dose-response curve. Each PaCa cell line was passaged with GEM at the IC_{50} concentration of the original cell line for 2 to 3 weeks. Following passage, the IC_{50} of the cell line to GEM was determined again. The PaCa cell lines were then passaged for 2 to 3 weeks with exposure to the IC_{50} concentration of the redetermined Gem. This process was repeated with increasing doses of GEM until the cell line exhibited an IC_{50} value to GEM that was at least 50-fold higher than that of the parental line.

Cell culture. Human PaCa cell lines (AsPC-1, BxPC-3, Capan2, MIA PaCa-2, PANC-1, and SW1990) and the immortalized human endothelial cell line EA.hy926 were purchased from American Type Culture Collection (ATCC). The human pancreatic ductal epithelial (HPDE) cell line H6C7 was purchased from Kerafast, Inc. AsPC-1, BxPC-3, Capan2, and EA.hy926 cells were maintained in RPMI-1640 medium (Sigma Aldrich; Merck KGaA). MIA PaCa-2, PANC-1, and SW1990 cells were maintained in Dulbecco's modified Eagle's medium (DMEM; Sigma Aldrich; Merck KGaA). H6C7 cells were maintained in keratinocyte serum-free medium (Gibco; Thermo Fisher Scientific, Inc.). Gem-R PaCa cell lines (MIA PaCa-2, AsPC-1), which were previously established and had been stored in liquid nitrogen, were used. Fetal bovine serum (FBS; 10%; Gibco; Thermo Fisher Scientific, Inc.) was added to both RPMI-1640 and DMEM. All media were supplemented with 10 mg/ml streptomycin, 10,000 U/ml penicillin, and 25 μg amphotericin B (Gibco; Thermo Fisher Scientific, Inc.). All cell lines were cultured at 37˚C in a humidified incubator containing 5% CO_2.

RNA interference. ILK small interfering RNA (siRNA; ID s7405: Sense, 5'-CGACCCAAAUUUGACAUGAtt-3' and antisense, 5'-UCAUGUCAAAUUUGGGUCGct-3') and nontargeted negative control siRNA (ncRNA; Silencer Select Negative Control No. 1; cat. no. 4390843; sequences not provided) were purchased from Thermo Fisher Scientific, Inc. PaCa cells were seeded in 6-well plates at 2.0×10^5 cells/well and cultured to 60% confluence before transfection with siRNA. According to the manufacturer's instructions, siRNA and Lipofectamine RNAiMAX (Invitrogen; Thermo Fisher Scientific, Inc.) were mixed in Opti-MEM (Invitrogen; Thermo Fisher Scientific, Inc.), and the mixture was then incubated at room temperature for 5 min. The siRNA-lipid complex was diluted in cell-appropriate medium to a final siRNA concentration of 10 nM. In the adjusted medium, the cells were cultured in a 5% CO_2 incubator at 37˚C for 24 h.

Reverse transcription-quantitative polymerase chain reaction (RT-qPCR). Total RNA was extracted from the samples used using QIAcube and RNeasy Plus Mini Kit (Qiagen GmbH) according to the manufacturer's protocol. Total RNA was then quantified using a NanoDrop 1000 (Thermo Fisher Scientific, Inc.). The RNA was then reverse transcribed using SuperScript III First-Strand Synthesis SuperMix (Invitrogen; Thermo Fisher Scientific, Inc.) and a T100 Thermal Cycler (Bio-Rad Laboratories, Inc.). The temperature protocol for reverse transcription was as follows: 25˚C for 10 min, 50˚C for 30 min, and 85˚C for 5 min. RT-qPCR was performed using TaqMan Gene Expression Assays (cat. no. 4331182; Applied Biosystems; Thermo Fisher Scientific, Inc.) and predesigned primers for *ILK* (Hs01101168_g1) and *Cxcl8* (Hs00174103_m1) from Thermo Fisher Scientific, Inc., on a CFX Connect Real-Time System (Bio-Rad Laboratories, Inc.). The thermocycling conditions were as follows: Initial denaturation at 95˚C for 20 sec, followed by 60 cycles at 95˚C for 1 sec and 60˚C for 20 sec. Glyceraldehyde 3-phosphate dehydrogenase (*GAPDH*; Hs99999905_m1; Thermo Fisher Scientific, Inc.) was used as a loading control to normalize mRNA levels, and samples were quantified using the standard curve method (16).

Western blotting. Proteins were extracted from cells using radioimmunoprecipitation lysis buffer containing Protease Inhibitor Single Use Cocktail and Phosphatase Inhibitor Cocktail (both Thermo Fisher Scientific, Inc.). Protein concentrations were measured using a Pierce BCA protein assay kit (Thermo Fisher Scientific, Inc.). Protein extracts (40 μg) were denatured at 90˚C for 5 min and separated on 10% Mini-PROTEAN TGX Precast gels (Bio-Rad Laboratories, Inc.). The protein bands were then transferred to nitrocellulose membranes and blocked in iBind Flex Solution (iBind Flex Buffer, iBind Flex Additive, and distilled water; Thermo Fisher Scientific, Inc.) for 20 min at room temperature. The primary and secondary antibody reactions were performed for 3 h at room temperature using the iBind Flex Western System (Thermo Fisher Scientific, Inc.) according to the manufacturer's instructions. The following primary antibodies were used: Anti-ILK antibody (1:1,000; cat. no. GTX101691; GeneTex, Inc.), anti-Akt (pan) (1:1,000; cat. no. 4691), anti-phoshorylated (p)-Akt (Ser473) (1:1,000; cat. no. 4060) and anti-GAPDH (1:1,000; cat. no. 2118; all from Cell Signaling Technology, Inc.). Horseradish peroxidase-conjugated goat anti-rabbit Polychronus (1:2,000; cat. no. P0448; DAKO; Agilent Technologies, Inc.) was used as the secondary antibody. The protein-antibody complexes were

visualized using SuperSignal West Femto Chemiluminescent Substrate or SuperSignal West PICO PLUS Chemiluminescent Substrate or Pierce ECL Western Blotting Substrate (Thermo Fisher Scientific, Inc.). Immunoreactive protein bands were detected using an Amersham Imager 600 (Cytiva), and the densities of the detected bands were calculated using ImageJ software 1.52v (National Institutes of Health).

Enzyme-linked immunosorbent assay (ELISA). Cells in the control group were seeded in 6-well plates in DMEM or RPMI-1640 medium appropriate for each cell line containing 5% FBS ($1.0x10^5$ cells/well). After overnight incubation, the medium was replaced (1 ml/well), and after 48 h, the culture supernatant was collected and centrifuged at 400 x g and 4˚C for 5 min to remove particulates. In the RNA transfection group, cells were collected 24 h after transfection and seeded into 6-well plates ($1.0x10^5$ cells/well). After overnight incubation, the medium was replaced (1 ml/well), and the culture supernatant was collected 48 h later. In the Cpd22 group, cells were pretreated with 1.0 μM Cpd22 for 48 h and seeded into 6-well plates ($1.0x10^5$ cells/well). After overnight incubation, the medium was replaced (1 ml/well), and the culture supernatant was collected 48 h later. The assay was performed using a Human IL-8/CXCL8 Quantikine ELISA Kit (cat. no. D8000C; R&D Systems, Inc.) with a SpectraMax ABS microplate reader (Molecular Devices, LLC). The concentration of each protein was determined according to the manufacturer's protocol.

Invasion assay. In vitro invasion assays were performed using Corning BioCoat Matrigel Invasion Chambers (Corning, Inc.) according to the manufacturer's protocol. Four groups of PaCa cell lines were used when suppressing ILK: Untreated PaCa cell lines, PaCa cell lines treated with siRNA or ncRNA, and PaCa cell lines treated with Cpd22. The PaCa cell lines were exposed to 1 μM of Cpd22 for 48 h. During Akt inhibition, untreated PaCa cell lines and PaCa cell lines treated with GSK690693 were used to evaluate invasive capacity. The PaCa cell lines were exposed to GSK690693 at 5 μM for 24 h. Cells were cultured at 5% CO_2 at 37˚C in all groups. Next, $1.0x10^5$ PaCa cells were conditioned in FBS-free medium and seeded in the upper chambers. The inducer used in the lower chamber was 10% FBS added to the medium. After 24 h of incubation at 37˚C, the top surface of the upper chamber was swabbed, and the invasive cells were fixed and stained using a Diff-Quick cell staining kit (Dade Behring), under room temperature, all samples were fixed for 10 sec and stained with two different staining solutions, each for 30 sec. The number of cells in nine randomly defined fields of view (magnification, x200) was counted under a light microscope.

Tube formation assay for analysis of angiogenesis. Tube formation was determined using angiogenesis assays with EA.hy926 cells and Matrigel (Corning, Inc.). Cells in the control group were seeded in 6-well plates ($1.0x10^5$ cells/well) using DMEM or RPMI-1640 medium containing 5% FBS, as appropriate for each cell line. After overnight incubation, the medium was replaced, and cells were incubated in medium containing 2% FBS for 48 h at 37˚C. In the RNA transfection group, cells were collected 48 h after transfection and seeded into 6-well plates ($1.0x10^5$ cells/well). In the Cpd22 group, cells were pretreated with 1.0 μM Cpd22 for 48 h and seeded into 6-well plates ($1.0x10^5$ cells/well). After overnight incubation, cells were replaced with medium containing 1% FBS (1 ml/well), and culture supernatants were collected 48 h later. The collected cell supernatants were centrifuged at 400 x g and 4˚C for 5 min, and particulates were discarded. Matrigel was added to a 96-well plate (50 μl/well), and the plates were incubated at 37˚C for 30 min to solidify the Matrigel. Next, EA.hy926 cells ($1.2x10^4$ cells/well) were added on top of the Matrigel. The cells were incubated in mixed medium (50 μl RPMI-1640 medium with 1% FBS and 50 μl/well of the aforementioned supernatant) for 16 h to form capillary-like structures; cells incubated in RPMI-1640 medium with 1% FBS alone served as controls. The number of endotubes was counted under a confocal microscope (magnification, x40), and 6 views per group were analyzed.

Statistical analysis. All statistical analyses were performed using EZR version 1.54 (Saitama Medical Center, Jichi Medical University, Saitama, Japan), which is a graphical user interface for R (The R Foundation for Statistical Computing). Data from experiments conducted at least in triplicate were expressed as the means ± standard deviations. Differences between the two samples were analyzed using unpaired t-tests. Comparisons of multiple groups were performed by one-way analysis of variance (ANOVA), and subsequent comparisons of individual groups were performed using post hoc Bonferroni tests; results with a P-value <0.05 were considered to indicate a statistically significant difference.

Results

ILK expression is upregulated in PaCa cells compared with HPDE cells. H6C7 is an immortalized epithelial cell line derived from normal HPDE cells. The expression of ILK in H6C7 and PaCa cell lines (AsPC-1, BxPC-3, Capan2, MIA PaCa-2, PANC-1, and SW1990) was evaluated using RT-qPCR and western blotting. *ILK* mRNA expression (Fig. 1A) was significantly higher in PaCa cells than in HPDE cells (P<0.05). Protein expression levels (Fig. 1B and C) were also significantly upregulated in PaCa cells, except for MIA PaCa-2 cells (P<0.05).

Changes in ILK expression levels after ILK knockdown in PaCa cell lines. RT-qPCR and western blotting were performed to evaluate changes in *ILK* mRNA expression in PaCa cell lines transfected with *ILK* siRNA. AsPC-1 and PANC-1 cells with high ILK expression were selected for *ILK* siRNA transfection. PaCa cell lines transfected with *ILK* siRNA exhibited significant downregulation of ILK compared with control cells or cells transfected with negative control siRNA (P<0.05; Fig. 2A and B).

Effects of ILK knockdown on PaCa cell invasion. Matrigel invasion assays were performed to evaluate the invasive potential of PaCa cell lines. Cell invasion ability was significantly suppressed in the ILK-knockdown group compared with that in the control and negative control groups (P<0.05; Fig. 2C and D).

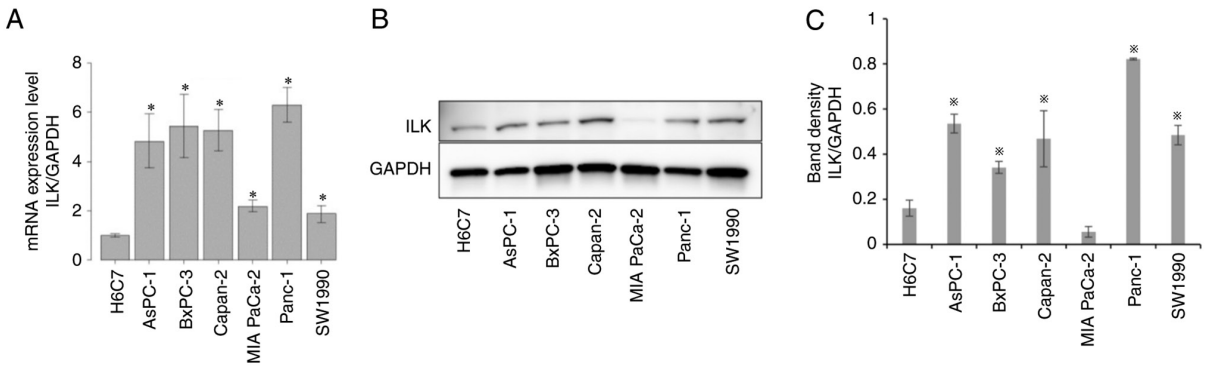

Figure 1. Comparison of ILK expression in human pancreatic ductal epithelial cells and PaCa cells. (A) ILK mRNA expression in HPDE cells (H6C7) and PaCa cells (AsPC-1, BxPC-3, Capan-2, MIA PaCa-2, PANC-1, SW1990) was assessed using reverse transcription-quantitative polymerase chain reaction. The mRNA expression status for each sample was normalized to the expression of *GAPDH*. (B) ILK protein expression levels in HPDE cells (H6C7) and PaCa cells (AsPC-1, BxPC-3, Capan-2, MIA PaCa-2, PANC-1, SW1990) were evaluated using western blotting. (C) The relative expression of ILK compared with GAPDH was assessed. Significant differences in ILK expression between HPDE (H6C7) and PaCa cells were assessed using one-way analysis of variance. *P<0.05. PaCa, pancreatic cancer; ILK, integrin-linked kinase.

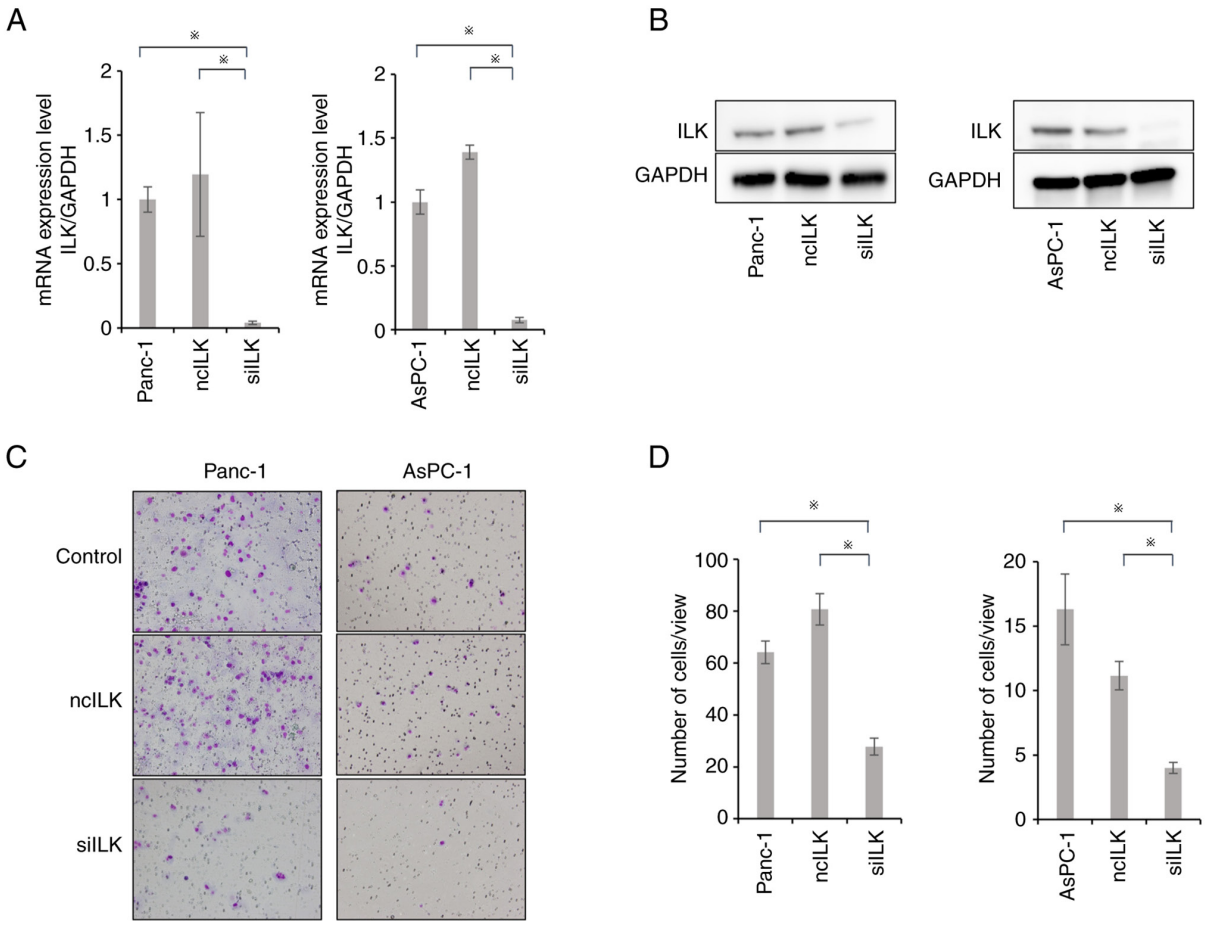

Figure 2. Changes in invasive potential following ILK knockdown in pancreatic cancer cell lines. (A) *ILK* mRNA expression following transfection with *ILK* siRNA was assessed using reverse transcription-quantitative polymerase chain reaction. (B) ILK protein expression after transfection with ILK siRNA was assessed using western blotting. (C and D) PaCa cells ($1.0x10^5$) were seeded into Matrigel-precoated Transwell chambers, and the number of invasive cells was determined after 24 h. Cells that passed through the Matrigel and invaded into the bottom of the upper chamber were fixed and stained using Diff-Quik staining. A comparison of the mean number of invasive cells in nine random microscopic fields of view is presented. Comparisons among groups were performed using one-way analysis of variance with post hoc Bonferroni tests. *P<0.05. ILK, integrin-linked kinase; siRNA, small interfering RNA; ncILK, negative control ILK; siILK, ILK siRNA.

Effects of ILK knockdown on the angiogenic potential of PaCa cell lines. The secretion of IL-8 as an angiogenic factor was evaluated by RT-qPCR and ELISA. *IL-8* mRNA expression and IL-8 secretion were significantly suppressed in the ILK-knockdown group compared with those in the control and negative control groups (P<0.05; Fig. 3A and B).

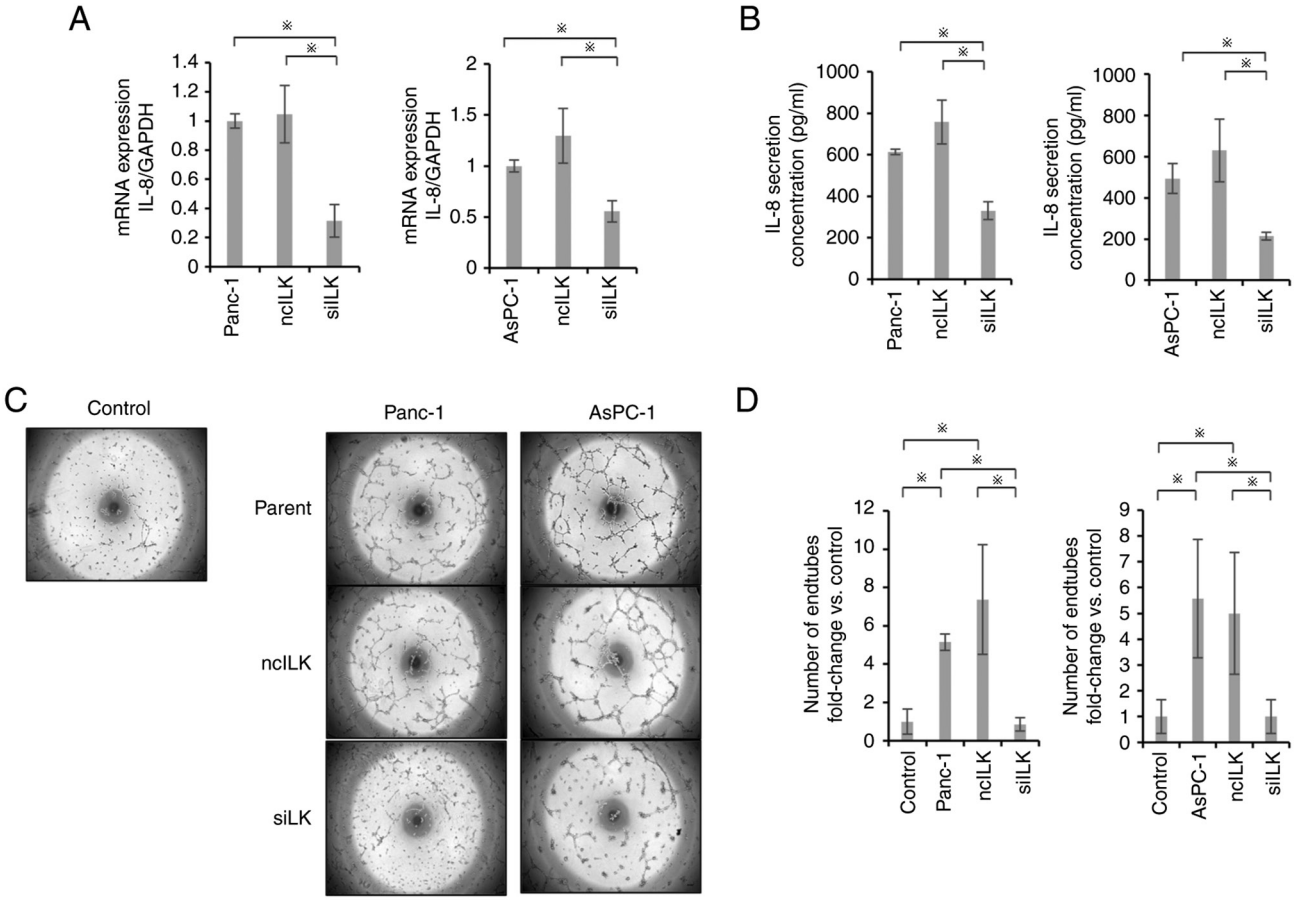

Figure 3. Changes in angiogenic potential following ILK knockdown in pancreatic cancer cell lines. (A) *IL-8* mRNA expression after transfection with *ILK* siRNA was assessed using reverse transcription-quantitative polymerase chain reaction. (B) IL-8 protein secretion following transfection with *ILK* siRNA was assessed using ELISA. (C and D) Angiogenic potential after transfection with *ILK* siRNA was determined using tube formation assays. EA.hy926 cells were seeded at $1.2x10^5$ cells/well and cultured with conditioned medium for 16 h. The control media was 1% RPMI-1640 containing FBS. The number of endotubes was counted, and differences among groups were evaluated using one-way analysis of variance with post hoc Bonferroni tests. *P<0.05. ILK, integrin-linked kinase; siRNA, small interfering RNA; ncILK, negative control ILK; siILK, ILK siRNA.

Tube formation assays also showed significant suppression in the ILK-knockdown group compared with the control and negative control groups (P<0.05; Fig. 3C and D).

Enhanced expression of ILK in Gem-R PaCa cells. RT-qPCR showed that *ILK* mRNA expression was significantly enhanced in Gem-R PaCa cells compared with Gem-sensitive (Gem-S) PaCa cells (P<0.05; Fig. 4A). Western blotting also confirmed that ILK protein expression was enhanced, consistent with the results of PCR (Fig. 4B).

Changes in ILK expression levels after ILK knockdown in Gem-R PaCa cell lines. RT-qPCR and western blotting were performed to assess changes in ILK expression in Gem-R PaCa cells transfected with *ILK* siRNA. *ILK* expression was downregulated in Gem-R PaCa cells transfected with *ILK* siRNA compared with that in control cells or cells transfected with negative control siRNA (P<0.05; Fig. 4C and D).

Enhanced invasive potential of Gem-R PaCa cells and effects of ILK knockdown on cell invasive potential. Matrigel invasion assays were performed to evaluate the invasive potential of Gem-R PaCa cells. Gem-R PaCa cells showed significantly higher invasive ability than Gem-S cells. Furthermore, *ILK* siRNA transfection inhibited the invasive ability, similar to that observed in Gem-S cells (P<0.05; Fig. 4E and F).

Angiogenic potential of Gem-R PaCa cells and effects of ILK knockdown. RT-qPCR and ELISA were used to evaluate IL-8 in Gem-R PaCa cells. Notably, Gem-R PaCa cells showed significantly higher *IL-8* mRNA expression and IL-8 protein secretion than Gem-S PaCa cells (P<0.05; Fig. 5A and B). Tube formation assays showed that tube formation was enhanced in Gem-R PaCa cells compared with that in Gem-S PaCa cells and was significantly suppressed in the ILK-knockdown group (P<0.05; Fig. 5C).

Effects of Cpd22 on proliferation in Gem-S and Gem-R PaCa cells. Gem-S and Gem-R PaCa cells were incubated with various concentrations of Cpd22 for 72 h, and the effects of Cpd22 on cell proliferation were then examined using WST-1 assays. Cpd22 inhibited proliferation in both Gem-R and Gem-S PaCa cell lines in a concentration-dependent manner. The IC_{50} values, as calculated from the WST-1 assay results, were as follows: 1.96 μM for PANC-1, 2.54 μM for SW1990, 2.05 μM for AsPC-1, and 2.16 μM for

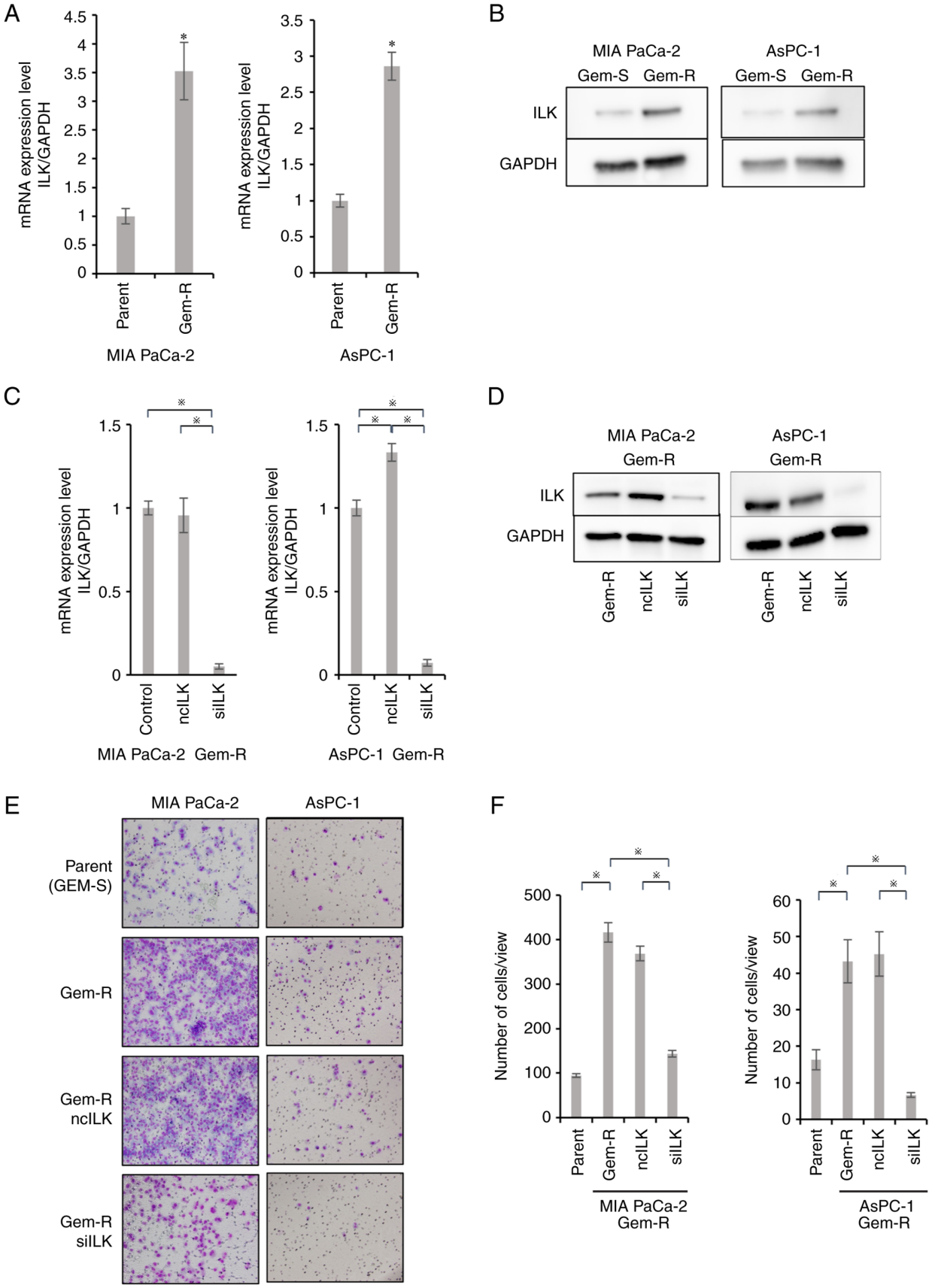

Figure 4. Comparison of ILK expression and invasive potential in Gem-S and Gem-R pancreatic cancer cell lines. (A) *ILK* mRNA expression in Gem-S and Gem-R PaCa cell lines (AsPC-1, MIA PaCa-2) was assessed using RT-qPCR. (B) ILK protein expression levels in Gem-S and Gem-R PaCa cell lines (AsPC-1, MIA PaCa-2) were assessed using western blotting. (C and D) RT-qPCR and western blotting were used to confirm ILK mRNA and protein expression following transfection with *ILK* siRNA. (E and F) The invasive ability of *ILK* siRNA-transfected Gem-R pancreatic cancer cells was evaluated as described in Fig. 3. Comparisons among groups was performed using one-way analysis of variance with post hoc Bonferroni tests. *P<0.05. ILK, integrin-linked kinase; Gem-S, Gem-sensitive; Gem-R, Gem-resistant; RT-qPCR, reverse transcription-quantitative polymerase chain reaction; siRNA, small interfering RNA; ncILK, negative control ILK; siILK, ILK siRNA.

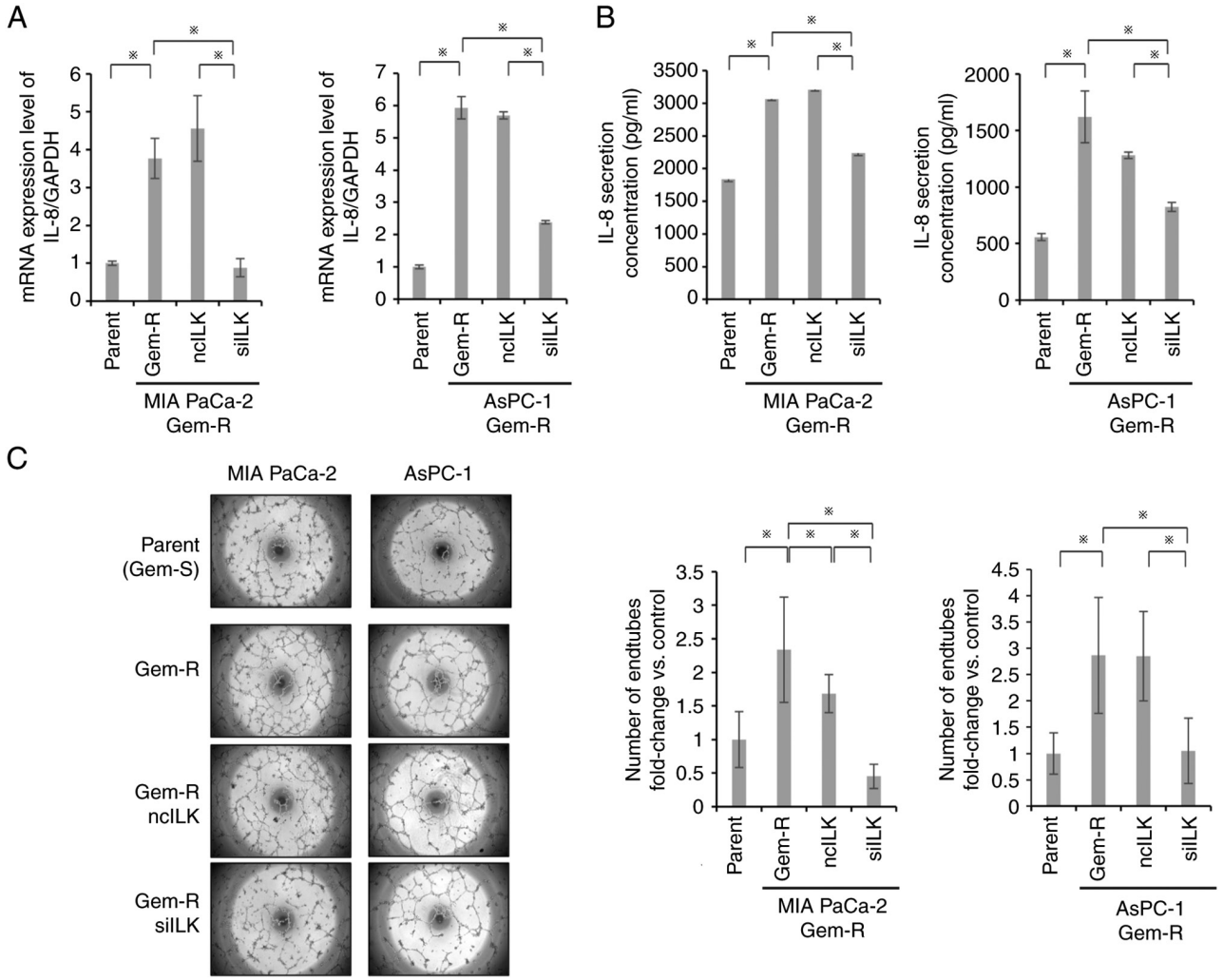

Figure 5. Changes in angiogenic potential following ILK knockdown in Gem-R (MIA PaCa-2, AsPC-1) PaCa cell lines. (A) *IL-8* mRNA expression after transfection with *ILK* siRNA was assessed using reverse transcription-quantitative polymerase chain reaction. (B) IL-8 secretion following transfection with *ILK* siRNA was measured using ELISA. (C) Angiogenic potential after transfection with *ILK* siRNA was assessed using Matrigel-based tube formation assays. Human endothelial cells (EAhy.926 cells) were seeded in Matrigel at 1.2×10^5 cells/well and cultured for 16 h in conditioned medium. The parental cell lines for Gem-R PaCa cell lines were used as controls. The number of endotubes was counted, and comparisons among groups were performed using one-way analysis of variance with post hoc Bonferroni tests. *P<0.05. ILK, integrin-linked kinase; Gem-R, Gem-resistant; siRNA, small interfering RNA; ncILK, negative control ILK; siILK, ILK siRNA.

MIA PaCa-2 (Fig. 6A and B). By contrast, the IC_{50} values for Gem-R AsPC-1 and Gem-R MIA PaCa-2 cells were 2.48 and 2.83 μM, respectively. To avoid the cytotoxic effects of Cpd22, the concentration of Cpd22 was set below the IC_{50} value in subsequent experiments.

Effects of Cpd22 on the drug sensitivity of Gem-R cells. Cpd22 was added to cells at 1 μM (a concentration that did not affect cell proliferation ability) in combination with Gem, and cells were cultured for 72 h. The sensitivity of AsPC-1 Gem-R cells to Gem increased from 787.4 to 363.6 nM, whereas that of MIA PaCA-2 Gem-R cells increased from 464.4 to 6.53 μM when Cpd22 was added (Fig. 6C and D).

Effects of Cpd22 on the invasive potential of PaCa cells. Matrigel invasion assays were performed to evaluate the invasive potential of PaCa cell lines via ILK suppression by Cpd22. In Gem-S and Gem-R PaCa cells (MIA PaCa-2, AsPC-1), cell invasion ability was significantly suppressed in the Cpd22 group compared with that in the untreated group (P<0.05; Fig. 7A).

Differences in the ILK/Akt pathway between Gem-S and Gem-R cells. Inhibition of ILK suppressed the phosphorylation of Akt at Ser473 in both Gem-S and Gem-R cell lines. The phosphorylation of Akt at Ser473 was significantly enhanced in Gem-R cells compared with that in Gem-S cells (P<0.05; Fig. 7B). The phosphorylation of Akt at Ser473, which was enhanced in Gem-R PaCa cells, was suppressed to the same extent as in the parental lines by inhibition of ILK.

Effect of GSK on the invasive potential of Gem-R PaCa cell lines. Matrigel invasion assay was performed to evaluate the invasive potential of PaCa cell lines via suppression of Akt by GSK. In Gem-R PaCa cells (MIA PaCa-2, AsPC-1), cell invasive potential was significantly suppressed in the GSK group compared to the untreated group (P<0.05; Fig. 7C).

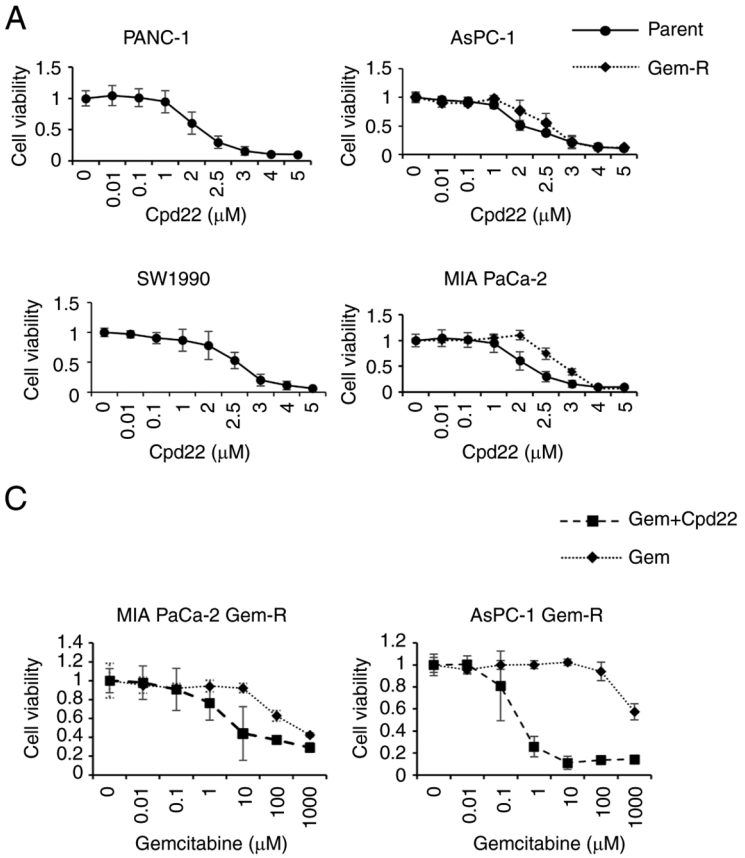

B

Cell line	IC_{50} for CpD22
AsPC-1 Gem-R	2.48 μM
AsPC-1 Parent	2.05 μM
MIA PaCa-2 Gem-R	2.83 μM
MIA PaCa-2 Parent	2.16 μM
PANC-1	1.96 μM
SW1990	2.54 μM

D

Cell line	IC_{50} for Gemcitabine
AsPC-1 Gem-R	787.4 μM
AsPC-1 Gem-R+Cpd22	363.6 μM
MIA PaCa-2 Gem-R	464.4 μM
MIA PaCa-2 Gem-R+Cpd22	6.53 μM

Figure 6. Inhibitory effects of Cpd22 on the proliferation of Gem-S (PANC-1, SW1990, AsPC-1, MIA PaCa-2) and Gem-R (AsPC-1, MIA PaCa-2) PaCa cell lines. (A) Cells were exposed to Cpd22 at the indicated concentrations for 48 h, and the degree of cell proliferation was evaluated using WST-1 assays. (B) IC_{50} values for Cpd22 were measured in PANC-1, SW1990, AsPC-1 Gem-S and Gem-R, and MIA PaCa-2 Gem-S and Gem-R cell lines. (C) Additive effects of Cpd22 on Gem sensitivity in Gem-R PaCa cells. Cells were exposed to Gem and 1 μM Cpd22 for 48 h, and the proliferation of each cell line was then evaluated using WST-1 assays. (D) The IC_{50} for Gem was measured in MIA-PaCa2 and AsPC-1 cells. Cpd22, compound 22; Gem, gemcitabine, Gem-S, gemcitabine-sensitive; Gem-R, gemcitabine-resistant, IC_{50}, half-maximal inhibitory concentration.

Effects of Cpd22 on the angiogenic potential of PaCa cells. RT-qPCR and ELISA were used to evaluate the effects of Cpd22-dependent ILK suppression on the secretory capacity of IL-8. In Gem-S cells, mRNA expression was significantly suppressed by Cpd22. IL-8 secretion was significantly suppressed in the Cpd22 group compared with that in the untreated group in MIA PaCa-2 and AsPC-1 cells ($P<0.05$; Fig. 8A and B). In Gem-R cells, both mRNA expression and protein secretion were suppressed. Tube formation assays also showed that angiogenesis was significantly suppressed in the Cpd22 group for both Gem-S and Gem-R cells ($P<0.05$; Fig. 8C).

Discussion

The aim of the present study was to clarify the roles of ILK in the resistance of PaCa cells to Gem and to determine whether Cpd22, an ILK inhibitor, exerted antitumor effects on Gem-S and Gem-R PaCa cells. The results of the present study confirmed that ILK was upregulated in Gem-R cells compared with that in Gem-S cells. Furthermore, invasion and angiogenesis assays demonstrated that invasive and angiogenic potentials were enhanced with ILK expression and that the malignant potential of the cells was increased. By contrast, inhibition of ILK expression suppressed invasiveness and angiogenesis in both Gem-S and Gem-R cells, and Cpd22, an ILK inhibitor, suppressed tumor growth, invasiveness, and angiogenesis in both Gem-S and Gem-R cells. The use of Cpd22 in addition to Gem improved Gem sensitivity in Gem-R cells. Overall, the findings of the present study also suggested that the degree of ILK expression contributed to malignancy in PaCa cells.

ILK has been demonstrated to interfere with the Akt, GSK-3β, and HIPPO pathways (17) and is involved in various mechanisms related to tumor progression, such as cell proliferation, apoptosis, invasion, and angiogenesis (9). Increased ILK expression has been reported in numerous malignant tumors, including lung (18), ovarian (19), colon (20,21), stomach (22), and liver cancers (23). Increased ILK expression may be associated with prognosis (8). The authors of the present study previously reported that ILK is significantly and strongly expressed in patients with PaCa and that high ILK expression and retroperitoneal invasion are poor prognostic factors (24). In the present study, it was determined that ILK expression tended to be higher in Gem-S PaCa cells than in HPDE cells. Moreover, ILK expression was even higher in more aggressive Gem-R PaCa cells than in Gem-S cells, providing support for the association between ILK and tumorgenicity.

The relationship between ILK and invasive potential has been discussed in previous studies. The invasive potential

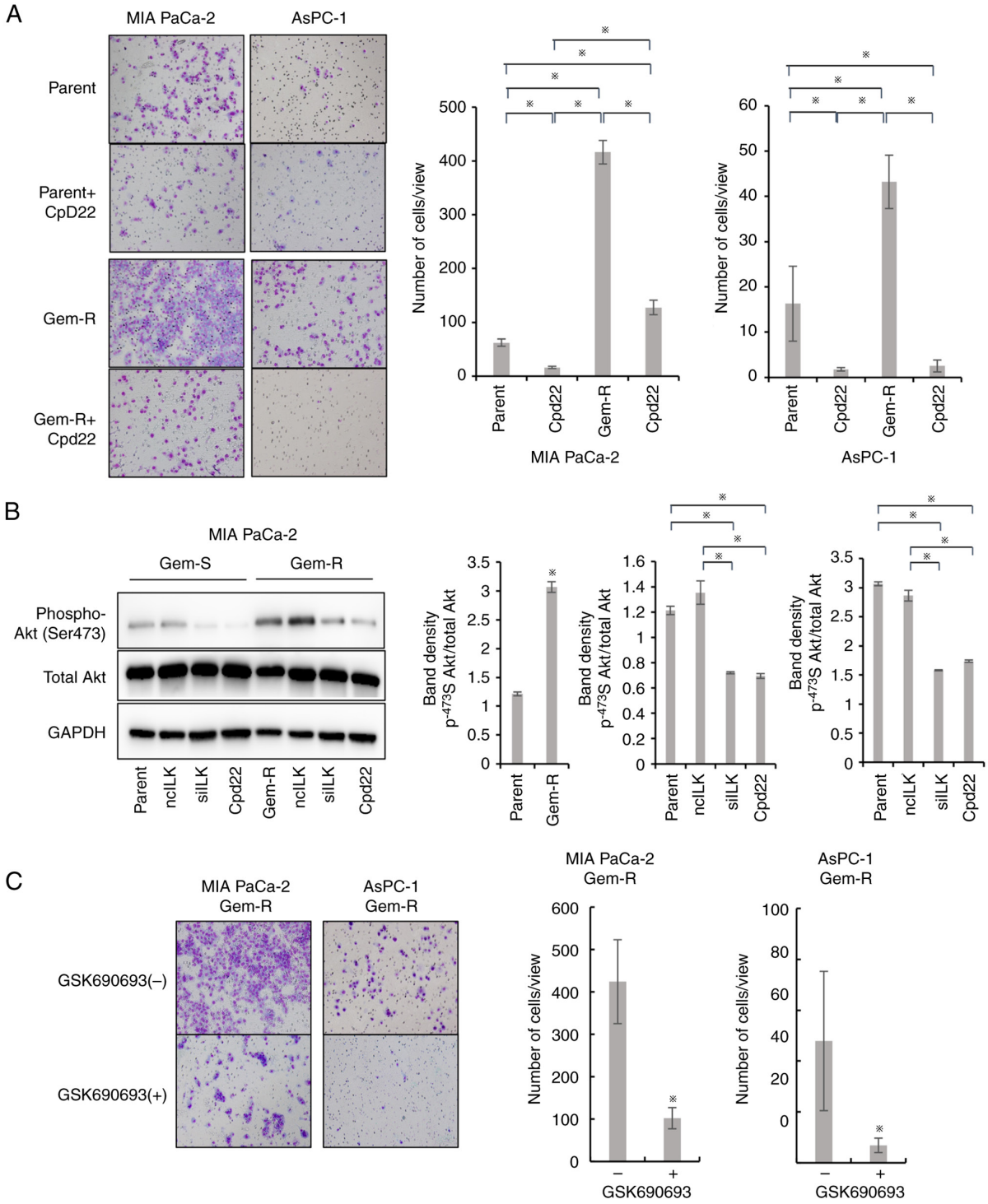

Figure 7. Changes in the invasive potential of Gem-S and Gem-R cell lines (AsPC-1, MIA PaCa-2) in response to inhibitor treatment were evaluated using Matrigel invasion assays. (A) Cells were pretreated with 1 μM Cpd22 for 48 h and then seeded at 1.0×10^5 cells/well in the upper chambers. The number of cells invading through the Matrigel was counted 24 h later. Representative images showing the invasion of Gem-S PaCa cells (AsPC-1 and MIA PaCa-2) and Gem-R PaCa cells (AsPC-1 and MIA PaCa-2) when Cpd22 was used. (B) MIA PaCa-2 Gem-S and Gem-R cell lysates were subjected to immunoblotting for assessment of changes in downstream signaling upon integrin-linked kinase inhibition. Cells were treated with Cpd22 for 12 h, and cell lysates were then harvested and immunoblotted for p-Akt (Ser473) and pan-Akt. GAPDH was used as a loading control. Data are presented as p-Akt (Ser473) levels relative to GAPDH expression. Comparisons among groups were performed using one-way analysis of variance with post hoc Bonferroni tests. *P<0.05. (C) Invasion assay was performed as in A. Cells were pretreated with 5 μM GSK69093 for 24 h before use. Representative images showing changes in invasion of Gem-R PaCa cells (AsPC-1 and MIA PaCa-2) when treated with GSK69093. Comparisons between the two groups were analyzed using the t-test. *P<0.05. Gem-S, Gem-sensitive; Gem-R, Gem-resistant; Cpd22, compound 22; p-, phosphorylated; ncILK, negative control ILK; siILK, ILK siRNA.

of PaCa is markedly high, resulting in low resectability rates. Additionally, ILK has been suggested to be involved in invasion through promotion of the EMT and lobular pseudopodia formation (7,9,25). ILK has also been demonstrated to be involved in invasion in PaCa cells (24). In the present study, ILK suppression in Gem-S PaCa cells blocked

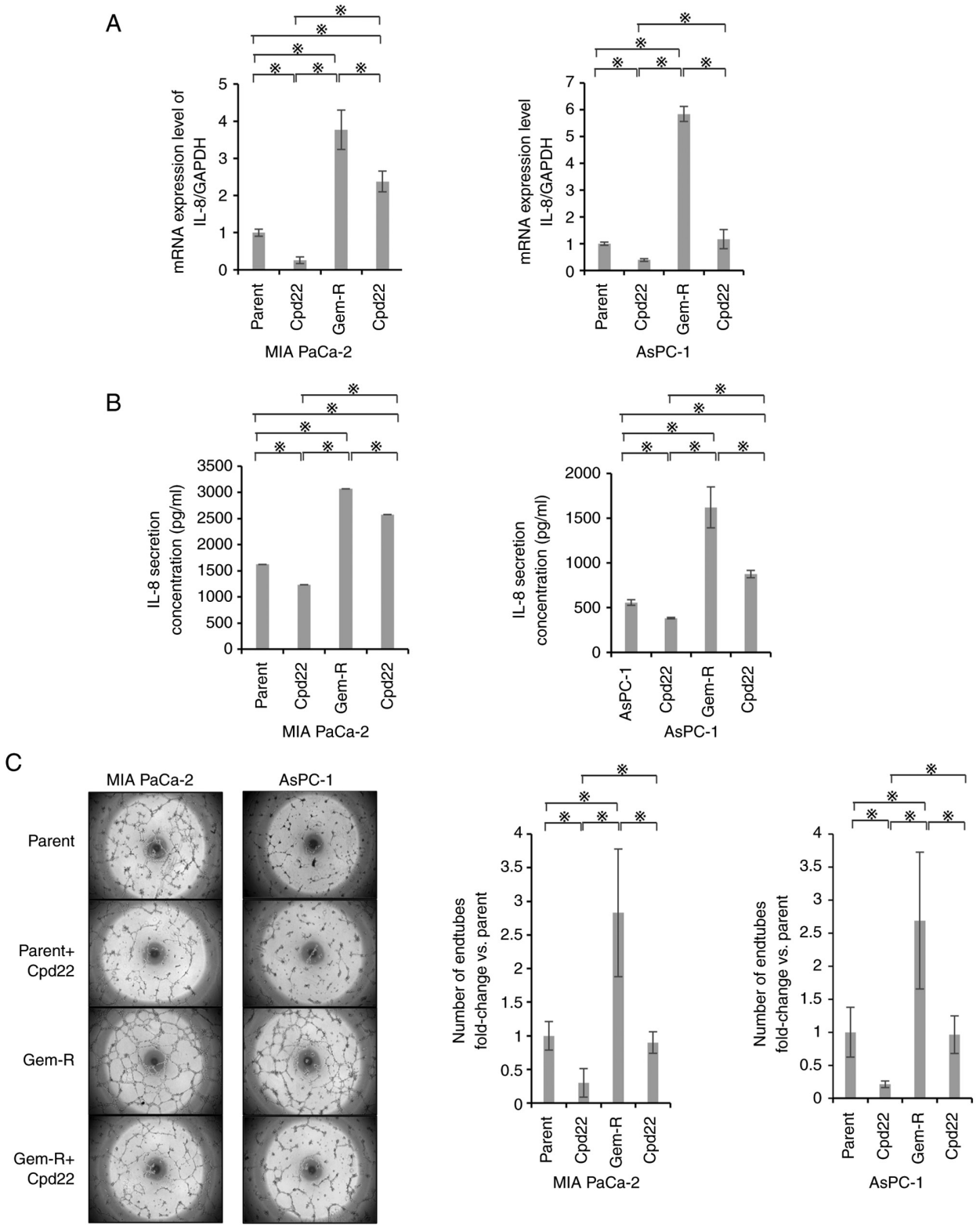

Figure 8. Changes in the angiogenic potential of Gem-S and Gem-R cell lines (AsPC-1, MIA PaCa-2) following Cpd22 treatment. (A) Alterations in *IL-8* mRNA expression in the presence of Cpd22 were assessed using reverse transcription-quantitative polymerase chain reaction. (B) Alterations in IL-8 secretion in the presence of Cpd22 were assessed using ELISA. (C) Changes in the angiogenic potential of Gem-S and Gem-R cell lines (AsPC-1, MIA PaCa-2) in the presence of Cpd22 were evaluated using tube formation assays with human endothelial cells. The number of endotubes was counted, and comparisons among groups were performed using one-way analysis of variance with post hoc Bonferroni tests. *P<0.05. Gem-S, Gem-sensitive; Gem-R, Gem-resistant; Cpd22, compound 22.

invasive potential, consistent with previous findings (24). Notably, invasive ability was enhanced in Gem-R PaCa cells in which ILK was upregulated compared with that in Gem-S PaCa cells. However, when ILK was suppressed, invasive ability was also inhibited to the same extent as that in Gem-S PaCa cells. It was also demonstrated that ILK

is likely to affect Akt to regulate invasive potential. The Akt pathway functions downstream of ILK (26,27). Akt is a signal transducer that is frequently activated in PaCa and is associated with tumor aggressiveness (28), and the relationship between the Akt pathway and tumor invasiveness is widely known. In the present study, it was determined that phosphorylation of Akt was enhanced in Gem-R PaCa cells in which ILK expression was upregulated compared with that in Gem-S PaCa cells. Furthermore, Akt phosphorylation was found to be suppressed to the same level as in Gem-S PaCa cells when ILK expression was suppressed. GSK690393 is an Akt inhibitor with strong selectivity for Akt kinase (29). To investigate whether inhibition of Akt can suppress the invasive potential of Gem-R PaCa cells with increased expression of ILK, the changes in invasive potential after exposure to GSK690393 were evaluated. Inhibition of Akt activity in the Gem-R PaCa cells suppressed invasive potential. While several pathways, including CXCL12/CXCR4 signaling (30) and NF-κB (31), as well as Akt, are reported to be involved in the invasive potential of cancer, the enhancement of the Akt pathway by upregulation of ILK may be involved in the enhancement of the invasive potential of Gem-R PaCa cells.

Subsequently, the angiogenic potential of the cells was evaluated. Several studies have shown that ILK promotes angiogenesis via vascular endothelial growth factor in cancer (32,33). PaCa, which is generally considered an ischemic tumor, has a high microvascular density, and the association between microvascular density and prognosis has been noted (34,35). It has been previously reported by the authors that IL-8 is involved in angiogenesis via the IL-8/CXCR2 axis in PaCa and that IL-8 expression is upregulated in Gem-R PaCa cell lines (15,36). In addition, Akt has been shown to be involved in the regulation of IL-8 (37,38). Therefore, the association between ILK and IL-8 were assessed and it was revealed that there was a relationship between the intensity of ILK/Akt pathway activity and the transcription and secretion of IL-8. Although further validation of the signaling pathway is required, the results of the present study suggest that ILK may be involved in the expression of IL-8 and may act to promote angiogenesis.

Cpd22, an ILK inhibitor, is a cell-permeable drug-like compound that has been reported to inhibit cell proliferation (IC_{50}, 1-2.5 μM) *in vitro* and to exert antiproliferative effects by inducing apoptosis. Cpd22 was revealed to block the Akt Ser473 phosphorylation, a downstream signal of ILK (9). In the present study, Cpd22 was used at the same concentration as previously reported and it was demonstrated that this concentration inhibited the proliferation of both Gem-R and Gem-S PaCa cells. Furthermore, Cpd22 inhibited the invasive and angiogenic potentials of these cell lines. Similar to the suppression of ILK expression using *ILK* siRNA, the suppression of ILK activity by Cpd22 was able to block the phosphorylation of Akt at Ser473.

ILK may be involved in chemotherapy resistance. In fact, ILK has been shown to be associated with the mechanism of chemotherapy resistance via the EMT, cancer stem cell markers, and the MRP1 pathway (6,39,40). In PaCa cells, ILK overexpression increases resistance to Gem chemotherapy by enhancing the phosphorylation of Akt and GSK-3β, whereas inhibition of ILK expression has been reported to induce Gem-induced apoptosis (5). Because activation of the Akt pathway resists apoptosis and phosphorylation of Akt is inhibited by Cpd22, the improved sensitivity may be the result of increased induction of apoptosis by Gem when used in combination with Cpd22. To the best of our knowledge, this is the first study to confirm the roles of ILK and the effects of ILK inhibitors using established Gem-R PaCa cells. The findings of the present study strongly indicated that Cpd22 exerted antitumor effects against PaCa cells and could be effective even after the cells acquired Gem resistance, supporting the potential application of Cpd22 as a novel therapeutic agent.

The present study had several limitations. Firstly, the behaviors of PaCa cell lines were not evaluated when ILK was overexpressed. In addition, animal studies are required to confirm the observed effects *in vivo*.

In conclusion, the results of the present study suggested that Gem-R PaCa cells exerted higher invasive and angiogenic potential and increased aggressiveness mediated by enhanced ILK/Akt signaling. Cpd22, an ILK inhibitor, suppressed the invasive and angiogenic potential of the cells and blocked cell proliferation in Gem-S and Gem-R PaCa cell lines. Cpd22 also enhanced Gem sensitivity in Gem-R cells. Therefore, Cpd22 may be an effective alternative therapy in patients with PaCa after acquisition of Gem resistance.

Acknowledgements

The authors would like to thank Ms Seiko Inumaru (Department of Gastroenterology, Nagoya City University Graduate School of Medicine, Nagoya, Japan), a laboratory assistant, for preparing the experimental reagents.

Funding

No funding was received.

Availability of data and materials

The data generated or analyzed in this study are included in the published article.

Authors' contributions

HM and YM contributed to the conception and design of this study, analyzed and interpreted the data, and wrote and reviewed the manuscript. HM, TK, YM, YH, HI, KS, MM, HT and ST were responsible for the design of this study. HM, TK, YA, YM, KN and YD acquired the data. TK, MK, AM and YM confirm the authenticity of all raw data. HM, YD, KN, YH, MM and RO wrote the Materials and methods section of the manuscript. YM, HT, RO and ST assisted in the technical, administrative, and material aspects of performing RT-qPCR, western blotting, and invasion assays. YM and ST provided technical, administrative, and material support. YM supervised the study. All authors have read the final manuscript and are equally responsible for all aspects of the study and guarantee its completeness and accuracy.

Ethics approval and consent to participate

Not applicable.

Patient consent for publication

Not applicable.

Competing interests

The authors declare that they have no competing interests.

References

1. Siegel RL, Miller KD, Fuchs HE and Jemal A: Cancer statistics, 2022. CA Cancer J Clin 72: 7-33, 2022.
2. Burris HA III, Moore MJ, Andersen J, Green MR, Rothenberg ML, Modiano MR, Cripps MC, Portenoy RK, Storniolo AM, Tarassoff P, *et al*: Improvements in survival and clinical benefit with gemcitabine as first-line therapy for patients with advanced pancreas cancer: A randomized trial. J Clin Oncol 15: 2403-2413, 1997.
3. Oettle H, Post S, Neuhaus P, Gellert K, Langrehr J, Ridwelski K, Schramm H, Fahlke J, Zuelke C, Burkart C, *et al*: Adjuvant chemotherapy with gemcitabine vs observation in patients undergoing curative-intent resection of pancreatic cancer: A randomized controlled trial. JAMA 297: 267-277, 2007.
4. Von Hoff DD, Ervin T, Arena FP, Chiorean EG, Infante J, Moore M, Seay T, Tjulandin SA, Ma WW, Saleh MN, *et al*: Increased survival in pancreatic cancer with nab-paclitaxel plus gemcitabine. N Engl J Med 369: 1691-1703, 2013.
5. Duxbury MS, Ito H, Benoit E, Waseem T, Ashley SW and Whang EE: RNA interference demonstrates a novel role for integrin-linked kinase as a determinant of pancreatic adenocarcinoma cell gemcitabine chemoresistance. Clin Cancer Res 11: 3433-3438, 2005.
6. Jia Z: Role of integrin-linked kinase in drug resistance of lung cancer. Onco Targets Ther 8: 1561-1565, 2015.
7. McDonald PC and Dedhar S: New perspectives on the role of integrin-linked kinase (ILK) signaling in cancer metastasis. Cancers (Basel) 14, 3209, 2022.
8. McDonald PC, Fielding AB and Dedhar S: Integrin-linked kinase-essential roles in physiology and cancer biology. J Cell Sci 121: 3121-3132, 2008.
9. Ning Z, Zhu X, Jiang Y, Gao A, Zou S, Gu C, He C, Chen Y, Ding WQ and Zhou J: Integrin-linked kinase is involved in the proliferation and invasion of esophageal squamous cell carcinoma. J Cancer 11: 324-333, 2020.
10. Ji C, Zhang M, Hu J, Cao C, Gu Q, Liu Y, Li X, Xu D, Ying L, Yang Y, *et al*: The kinase activity of integrin-linked kinase regulates cellular senescence in gastric cancer. Cell Death Dis 13: 577, 2022.
11. Li B, Wang X, Wang R, Rutz B, Ciotkowska A, Gratzke C, Herlemann A, Spek A, Tamalunas A, Waidelich R, *et al*: Inhibition of neurogenic and thromboxane A_2-induced human prostate smooth muscle contraction by the integrin $\alpha 2\beta 1$ inhibitor BTT-3033 and the integrin-linked kinase inhibitor Cpd22. Prostate 80: 831-849, 2020.
12. Sarı Kılıçaslan SM and İncesu Z: Effects of integrin-linked kinase on protein kinase b, glycogen synthase kinase-3β, and β-catenin molecules in ovarian cancer cells. Iran J Basic Med Sci 24: 1500-1508, 2021.
13. Yau CY, Wheeler JJ, Sutton KL and Hedley DW: Inhibition of integrin-linked kinase by a selective small molecule inhibitor, QLT0254, inhibits the PI3K/PKB/mTOR, Stat3, and FKHR pathways and tumor growth, and enhances gemcitabine-induced apoptosis in human orthotopic primary pancreatic cancer xenografts. Cancer Res 65: 1497-1504, 2005.
14. Zeng S, Pöttler M, Lan B, Grützmann R, Pilarsky C and Yang H: Chemoresistance in Pancreatic Cancer. Int J Mol Sci 20: 4504, 2019.
15. Imafuji H, Matsuo Y, Ueda G, Omi K, Hayashi Y, Saito K, Tsuboi K, Morimoto M, Koide S, Ogawa R, *et al*: Acquisition of gemcitabine resistance enhances angiogenesis via upregulation of IL8 production in pancreatic cancer. Oncol Rep 41: 3508-3516, 2019.
16. Bustin SA: Quantification of mRNA using real-time reverse transcription PCR (RT-PCR): trends and problems. J Mol Endocrinol 29: 23-39, 2002.
17. Serrano I, McDonald PC, Lock F, Muller WJ and Dedhar S: Inactivation of the Hippo tumour suppressor pathway by integrin-linked kinase. Nat Commun 4: 2976, 2013.
18. Takanami I: Increased expression of integrin-linked kinase is associated with shorter survival in non-small cell lung cancer. BMC Cancer 5: 1, 2005.
19. Ahmed N, Riley C, Oliva K, Stutt E, Rice GE and Quinn MA: Integrin-linked kinase expression increases with ovarian tumour grade and is sustained by peritoneal tumour fluid. J Pathol 201: 229-237, 2003.
20. Marotta A, Parhar K, Owen D, Dedhar S and Salh B: Characterisation of integrin-linked kinase signalling in sporadic human colon cancer. Br J Cancer 88: 1755-1762, 2003.
21. Bravou V, Klironomos G, Papadaki E, Stefanou D and Varakis J: Integrin-linked kinase (ILK) expression in human colon cancer. Br J Cancer 89: 2340-2341, 2003.
22. Ito R, Oue N, Zhu X, Yoshida K, Nakayama H, Yokozaki H and Yasui W: Expression of integrin-linked kinase is closely correlated with invasion and metastasis of gastric carcinoma. Virchows Arch 442: 118-123, 2003.
23. Peroukides S, Bravou V, Varakis J, Alexopoulos A, Kalofonos H and Papadaki H: ILK overexpression in human hepatocellular carcinoma and liver cirrhosis correlates with activation of Akt. Oncol Rep 20: 1337-1344, 2008.
24. Sawai H, Okada Y, Funahashi H, Matsuo Y, Takahashi H, Takeyama H and Manabe T: Integrin-linked kinase activity is associated with interleukin-1 alpha-induced progressive behavior of pancreatic cancer and poor patient survival. Oncogene 25: 3237-3246, 2006.
25. Canel M, Serrels A, Frame MC and Brunton VG: E-cadherin-integrin crosstalk in cancer invasion and metastasis. J Cell Sci 126: 393-401, 2013.
26. Troussard AA, Mawji NM, Ong C, Mui A, St–Arnaud R and Dedhar S: Conditional knock-out of integrin-linked kinase demonstrates an essential role in protein kinase B/Akt activation. J Biol Chem 278: 22374-22378, 2003.
27. Qu Y, Hao C, Xu J, Cheng Z, Wang W and Liu H: ILK promotes cell proliferation in breast cancer cells by activating the PI3K/Akt pathway. Mol Med Rep 16: 5036-5042, 2017.
28. Schlieman MG, Fahy BN, Ramsamooj R, Beckett L and Bold RJ: Incidence, mechanism and prognostic value of activated AKT in pancreas cancer. Br J Cancer 89: 2110-2115, 2003.
29. Heerding DA, Rhodes N, Leber JD, Clark TJ, Keenan RM, Lafrance LV, Li M, Safonov IG, Takata DT, Venslavsky JW, *et al*: Identification of 4-(2-(4-amino-1,2,5-oxadiazol-3-yl)-1-ethyl-7-{[(3S)-3-piperidinylmethyl]oxy}-1H-imidazo[4,5-c] pyridin-4-yl)-2-methyl-3-butyn-2-ol (GSK690693), a novel inhibitor of AKT kinase. J Med Chem 51: 5663-5679, 2008.
30. Kato T, Matsuo Y, Ueda G, Murase H, Aoyama Y, Omi K, Hayashi Y, Imafuji H, Saito K, Morimoto M, *et al*: Enhanced CXCL12/CXCR4 signaling increases tumor progression in radiation-resistant pancreatic cancer. Oncol Rep 47: 68, 2022.
31. Maier HJ, Schmidt-Strassburger U, Huber MA, Wiedemann EM, Beug H and Wirth T: NF-kappaB promotes epithelial-mesenchymal transition, migration and invasion of pancreatic carcinoma cells. Cancer Lett 295: 214-228, 2010.
32. Zheng CC, Hu HF, Hong P, Zhang QH, Xu WW, He QY and Li B: Significance of integrin-linked kinase (ILK) in tumorigenesis and its potential implication as a biomarker and therapeutic target for human cancer. Am J Cancer Res 9: 186-197, 2019.
33. Tan C, Cruet-Hennequart S, Troussard A, Fazli L, Costello P, Sutton K, Wheeler J, Gleave M, Sanghera J and Dedhar S: Regulation of tumor angiogenesis by integrin-linked kinase (ILK). Cancer Cell 5: 79-90, 2004.
34. Stipa F, Lucandri G, Limiti MR, Bartolucci P, Cavallini M, Di Carlo V, D'Amato A, Ribotta G and Stipa S: Angiogenesis as a prognostic indicator in pancreatic ductal adenocarcinoma. Anticancer Res 22: 445-449, 2002.
35. Benckert C, Thelen A, Cramer T, Weichert W, Gaebelein G, Gessner R and Jonas S: Impact of microvessel density on lymph node metastasis and survival after curative resection of pancreatic cancer. Surg Today 42: 169-176, 2012.
36. Matsuo Y, Ochi N, Sawai H, Yasuda A, Takahashi H, Funahashi H, Takeyama H, Tong Z and Guha S: CXCL8/IL-8 and CXCL12/SDF-1alpha co-operatively promote invasiveness and angiogenesis in pancreatic cancer. Int J Cancer 124: 853-861, 2009.

37. Grzesiak JJ, Smith KC, Burton DW, Deftos LJ and Bouvet M: GSK3 and PKB/Akt are associated with integrin-mediated regulation of PTHrP, IL-6 and IL-8 expression in FG pancreatic cancer cells. Int J Cancer 114: 522-530, 2005.
38. Wang L, Tang C, Cao H, Li K, Pang X, Zhong L, Dang W, Tang H, Huang Y, Wei L, *et al*: Activation of IL-8 via PI3K/Akt-dependent pathway is involved in leptin-mediated epithelial-mesenchymal transition in human breast cancer cells. Cancer Biol Ther 16: 1220-1230, 2015.
39. Tsoumas D, Nikou S, Giannopoulou E, Champeris Tsaniras S, Sirinian C, Maroulis I, Taraviras S, Zolota V, Kalofonos HP and Bravou V: ILK Expression in colorectal cancer is associated with EMT, Cancer stem cell markers and chemoresistance. Cancer Genomics Proteomics 15: 127-141, 2018.
40. Zheng X, Carstens JL, Kim J, Scheible M, Kaye J, Sugimoto H, Wu CC, LeBleu VS and Kalluri R: Epithelial-to-mesenchymal transition is dispensable for metastasis but induces chemoresistance in pancreatic cancer. Nature 527: 525-530, 2015.